

Notch ligand Delta-like 4 blockade attenuates atherosclerosis and metabolic disorders

Daiju Fukuda^a, Elena Aikawa^a, Filip K. Swirski^b, Tatiana I. Novobrantseva^c, Victor Kotelianski^c, Cem Z. Gorgun^d, Aleksey Chudnovskiy^b, Hiroyuki Yamazaki^a, Kevin Croce^a, Ralph Weissleder^b, Jon C. Aster^e, Gökhan S. Hotamisligil^d, Hideo Yagita^f, and Masanori Aikawa^{a,1}

Departments of ^aMedicine and ^ePathology, Brigham and Women's Hospital, Harvard Medical School, Boston, MA 02115; ^bCenter for Systems Biology, Massachusetts General Hospital, Harvard Medical School, Boston, MA 02114; ^cDepartment of Research, Alnylam Pharmaceuticals, Cambridge, MA 02142; ^dDepartment of Genetics and Complex Diseases, Harvard School of Public Health, Boston, MA 02115; and ^fDepartment of Immunology, Juntendo University School of Medicine, Tokyo 113, Japan

Edited by Monty Krieger, Massachusetts Institute of Technology, Cambridge, MA, and approved May 11, 2012 (received for review October 18, 2011)

Atherosclerosis and insulin resistance are major components of the cardiometabolic syndrome, a global health threat associated with a systemic inflammatory state. Notch signaling regulates tissue development and participates in innate and adaptive immunity in adults. The role of Notch signaling in cardiometabolic inflammation, however, remains obscure. We noted that a high-fat, high-cholesterol diet increased expression of the Notch ligand Delta-like 4 (Dll4) in atheromata and fat tissue in LDL-receptor-deficient mice. Blockade of Dll4-Notch signaling using neutralizing anti-Dll4 antibody attenuated the development of atherosclerosis, diminished plaque calcification, improved insulin resistance, and decreased fat accumulation. These changes were accompanied by decreased macrophage accumulation, diminished expression of monocyte chemoattractant protein-1 (MCP-1), and lower levels of nuclear factor- κ B (NF- κ B) activation. In vitro cell culture experiments revealed that Dll4-mediated Notch signaling increases MCP-1 expression via NF- κ B, providing a possible mechanism for in vivo effects. Furthermore, Dll4 skewed macrophages toward a proinflammatory phenotype ("M1"). These results suggest that Dll4-Notch signaling plays a central role in the shared mechanism for the pathogenesis of cardiometabolic disorders.

biotherapy | cardiovascular diseases | collagen | diabetes mellitus | obesity

Atherosclerosis and insulin resistance are cardinal features of the so-called cardiometabolic syndrome, a global health threat (1). Although chronic inflammation strongly associates with major components of this syndrome (2), the underlying proinflammatory mechanisms are incompletely understood. The Notch pathway regulates embryonic development (3) and contributes to physiological homeostasis and pathological processes in adult tissues (4–7). Notch receptors (Notch1–4) undergo proteolytic cleavage when bound by Delta-like (Dll1, Dll3, Dll4) or Serrate (Jagged1, Jagged2) ligands expressed on adjacent cells, allowing nuclear translocation of the Notch intracellular domain. Notch pathway components are expressed in a cell-type-specific fashion and have diverse context-dependent functions. Among previous studies on diverse roles of Notch signaling in physiology and pathology, recent reports have suggested that Notch signaling has metabolic functions and that Notch inhibition is beneficial in the treatment for insulin resistance (8, 9). Dll4, originally found as an endothelial cell-specific ligand, participates in angiogenesis and may be a therapeutic target for solid tumors (10–12). However, the role of Dll4 in cardiometabolic inflammation remains unknown. We showed previously that Dll4-triggered Notch signaling promotes inflammatory responses in macrophages in vitro (13). Macrophages play pivotal roles in the development of chronic inflammatory diseases. We therefore tested the hypothesis in vivo that Dll4 contributes to the pathogenesis of the cardiometabolic syndrome.

In this study, we blocked Dll4-mediated Notch signaling using a previously described neutralizing anti-mouse Dll4 antibody (Ab) (14–20) in LDL-receptor-deficient (*Ldlr*^{-/-}) mice fed a high-fat, high-cholesterol diet, a model that produces atherosclerosis

and metabolic disturbances resembling those seen in the cardiometabolic syndrome (21). Generation of anti-mouse Dll4 Ab was described in previous studies (14, 17). Previous studies thoroughly characterized the same Ab (14–20). The selective binding of the Ab (HMD4-2) to mouse Dll4 was verified by flow cytometry, using mouse Dll4-expressing cells (14). The Ab blocks Notch1-Fc and Notch4-Fc binding to mouse Dll4-expressing cells in a dose-dependent manner and does not bind to cells expressing other mouse Notch ligands, such as Dll1, Jagged1, or Jagged2 (14, 17). Other reports demonstrated that the Ab blocked Dll4-dependent Notch signaling in vivo, using cancer transplant models (17, 20). Use of anti-Dll4 Ab enabled us to circumvent the embryonic lethality of Dll4 deficiency (22), and to provide clinically translatable evidence for the proinflammatory role of Dll4. Multiple cellular and molecular pathways associate with the pathogenesis of cardiometabolic disorders. Although our approach did not aim to examine the relative contribution of metabolic cell types, in vivo and in vitro experiments in this study addressed the function of Dll4 in each cell type, proposing the shared mechanisms by which Dll4-mediated Notch signaling promotes cardiometabolic diseases. This study demonstrates unique in vivo evidence that Dll4-mediated Notch signaling contributes to the pathogenesis of cardiometabolic disorders and provides proof of concept that the Notch pathway is a new target for much-needed therapies against the cardiometabolic syndrome.

Results

Characterization of Dll4 Expression and the Effects of Neutralizing Anti-Dll4 Ab. Atherosclerotic lesions and epididymal adipose tissue of 32-wk-old *Ldlr*^{-/-} mice fed a high-fat, high-cholesterol diet contained immunoreactive Dll4, as did human white adipose tissue (Fig. 1A) and atheromata, as described previously (13). Dll4 protein and RNA levels increased in the aorta and adipose tissue, compared with levels in wild-type mice (Fig. 1B and C). Furthermore, high-fat feeding promoted Dll4 expression in these organs in a time-dependent manner (Fig. 1D and E). These results suggest that an inflammatory environment triggered by overnutrition promotes Dll4 expression in vivo. Bolus injection of Dll4 Ab (250 μ g) into *Ldlr*^{-/-} mice significantly reduced the expression of the prototypical Notch target gene *Hes1* in peritoneal macrophages and of *Hes1* and *Hey1* in fat (SI Appendix, Fig. S1A), indicating that the Notch pathway is activated by Dll4 in important cardiometabolic organs. In addition, Dll4 Ab

Author contributions: D.F., F.K.S., and M.A. designed research; D.F., E.A., F.K.S., T.I.N., V.K., C.Z.G., A.C., H. Yamazaki, K.C., G.S.H., and M.A. performed research; R.W. and H. Yagita contributed new reagents/analytic tools; D.F., E.A., F.K.S., T.I.N., V.K., C.Z.G., A.C., K.C., J.C.A., G.S.H., and M.A. analyzed data; and D.F., E.A., K.C., J.C.A., G.S.H., and M.A. wrote the paper.

The authors declare no conflict of interest.

This article is a PNAS Direct Submission.

¹To whom correspondence should be addressed. E-mail: maikawa@rics.bwh.harvard.edu.

See Author Summary on page 10763 (volume 109, number 27).

This article contains supporting information online at www.pnas.org/lookup/suppl/doi:10.1073/pnas.1116889109/-DCSupplemental.

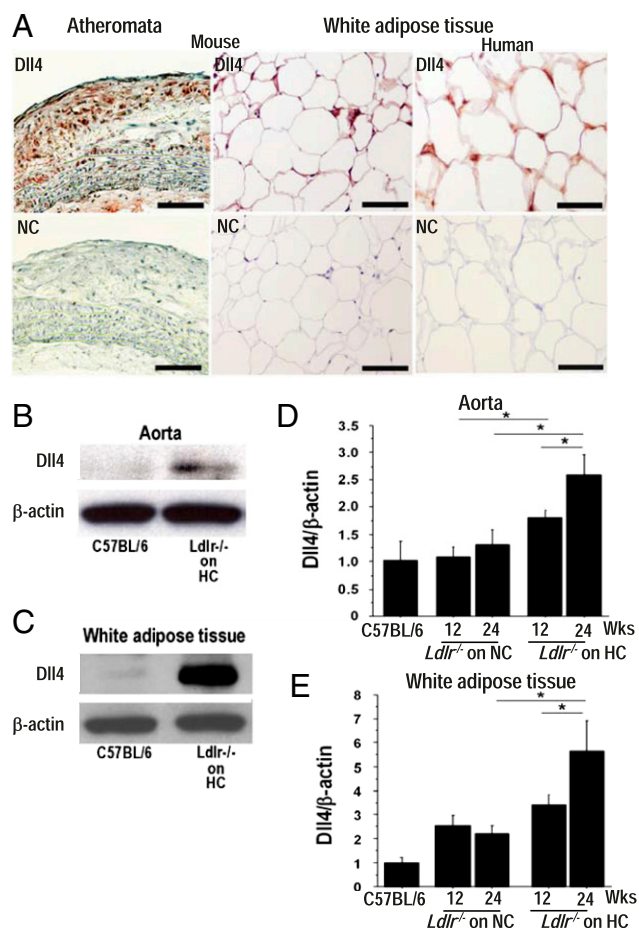


Fig. 1. Characterization of Dll4 expression and effects of Dll4 blockade. (A) Immunostaining of Dll4 in atheroma (Upper Left) and epididymal fat (Upper Center) obtained from 32-wk-old *Ldlr*^{-/-} mice on a high-fat and high-cholesterol (HC) diet and in human white adipose tissue (Upper Right). (Lower) Staining with nonimmune IgG (NC). (Scale bar: 100 μ m.) (B and C) Immunoblotting of Dll4 in aortas (B) and white adipose tissue (C). (D and E) Effect of HC diet on Dll4 RNA expression in aortas (D) and adipose tissue (E) of *Ldlr*^{-/-} mice. Mice were fed a HC diet from 8 wk of age for 12 or 24 wk. HC diet promotes Dll4 expression. Longer consumption of HC diet enhances the effect. NC, normal chow. A and B, $n = 4$. D and E, $n = 4$. * $P < 0.05$; ** $P < 0.01$. All values are mean \pm SEM.

inhibited Notch signaling in Notch reporter transgenic mice (23) (SI Appendix, Fig. S1B). As mentioned above, previous studies verified the specificity of the same Dll4 blocking Ab (14–20).

To investigate the role of Dll4–Notch signaling in the initiation and progression of cardiometabolic disorders, we intraperitoneally administered Dll4 Ab or isotype control IgG (250 μ g, twice a week) for 12 wk to fat-fed *Ldlr*^{-/-} mice beginning at 8 wk of age (early-phase treatment) or at 20 wk of age (late-phase treatment), respectively (SI Appendix, Fig. S1C). Unlike pan-Notch inhibitors (e.g., γ -secretase inhibitors), which cause severe and potentially fatal gut toxicity and thymus atrophy (24), our Dll4 Ab did not exert any obvious adverse effects and was well tolerated (SI Appendix, Fig. S1D and E).

Dll4 Blockade Reduces Atherogenesis. Dll4 blockade lessened the severity of atherosclerotic lesions in two vascular beds where atherosclerotic changes often develop in hyperlipidemic mice—the aorta (Fig. 2) and brachiocephalic artery (SI Appendix, Fig. S2). Both early-phase and late-phase Dll4 Ab-treated mice showed milder stenosis of brachiocephalic arteries, whereas late-phase treatment reduced the size of atherosclerotic lesions in the aortic arch (Fig. 24). Dll4 Ab treatment markedly decreased

monocyte chemoattractant protein-1 (MCP-1) expression (Fig. 2B and SI Appendix, Fig. S24) and macrophage accumulation (Fig. 2C and SI Appendix, Fig. S2B) in atherosclerotic lesions in the aorta and brachiocephalic artery. MCP-1 immunoreactivity was also lower in the tunica media of the Ab-treated mice, indicating that Dll4 blockade may suppress MCP-1 expression in smooth muscle cells.

We and others have established the role of macrophage-derived proteinases, including matrix metalloproteinases (MMP), in collagen degradation—which can lead to atherosclerotic plaque “instability” and acute vascular events (25, 26). Dll4 Ab-treated mice demonstrated increased fibrillar collagen in atherosclerotic plaques (Fig. 2D and SI Appendix, Fig. S3C). Several studies, including ours, have shown that macrophages promote arterial calcification (27–29), and other evidence indirectly suggests that Notch signaling also regulates calcification (30). Ab treatment significantly decreased advanced calcification (von Kossa) and osteogenic activity (alkaline phosphatase activity, ALP) in atherosclerotic lesions (Fig. 2E and F and SI Appendix, Fig. S3D and E). Molecular imaging using fluorescence reflectance demonstrated that macrophage-targeted signal correlated positively with osteogenic activity, and that both of these features decreased with Dll4 Ab treatment in parallel (Fig. 2G). A recent study by Feig et al. reported that changes in total plaque area do not follow the monotonic decline in macrophages and that the potential underlying mechanisms may involve increased plaque collagen, which was observed in our Ab-treated animals (31). Our present results are consistent with this report. Furthermore, clinical evidence suggests that inflammation, rather than atheroma size, participates critically in plaque instability and acute complications, and that antiinflammatory therapies such as lipid lowering attenuate macrophage burden and collagen loss and improve clinical outcomes, even though they may not substantially shrink lesions (26). We therefore believe that our results provide clinically relevant information on the effects of Dll4 Ab administration on an inflammatory plaque phenotype.

Calcific aortic valve disease, an inflammatory disorder, causes aortic stenosis and heart failure and is a major burden in clinical practice (32). Dll4 blockade trended toward a decrease in the thickness of aortic valve leaflets (40.0 ± 2.7 vs. 32.5 ± 2.7 μ m, $P = 0.06$) and in osteogenic activity detected by ALP activity and molecular imaging (Fig. 2H and I). Whereas Dll4 blockade suppressed ectopic cardiovascular calcification, it did not decrease bone mineral density (SI Appendix, Fig. S3A).

Consistent with reduced calcification, Dll4 Ab treatment tended to decrease aortic expression of osteogenic regulators and bone morphogenetic proteins (BMPs) (Fig. 3A and B). Dll4 Ab treatment also reduced the expression of MMP-9 and MMP-13, enzymes responsible for collagen degradation in plaques (33) (Fig. 3C). Furthermore, the expression of proinflammatory mediators, including IL-1 β , iNOS, and IL-6, was generally lower in the aortas of Ab-treated mice than in those of control mice (Fig. 3D). Dll4 Ab also decreased aortic expression of the Notch target gene *Hey2*, consistent with effective blockade of Notch signaling in this tissue (SI Appendix, Fig. S4A). In addition, Dll4 Ab decreased the expression of BMP-2 and MMP-9 in peritoneal macrophages (Fig. 3E and F). To evaluate further whether blockade of Dll4 signaling in macrophages mediated effects on MMP expression in the aorta, *in vitro* experiments used the murine macrophage-like cell line RAW264.7. siRNA against Dll4 reduced MMP-9 expression, whereas overexpression of Dll4 or exogenous immobilized recombinant Dll4 (34) tended to increase MMP-9 expression ($P = 0.07$ and 0.09 , respectively) (SI Appendix, Fig. S3B–D).

Dll4 Blockade Retards Excessive Fat Accumulation. Body weight gain in *Ldlr*^{-/-} mice was similar in Dll4 Ab and IgG groups during early-phase treatment (8–20 wk of age), which was equivalent to that of the nontreatment period in the late-phase treatment protocol (from 8 to 20 wk of age). Late-phase Dll4 Ab treatment (from 20 to 32 wk of age), however, retarded excessive body weight gain (Fig. 44). Dll4 Ab reduced fat and liver weight

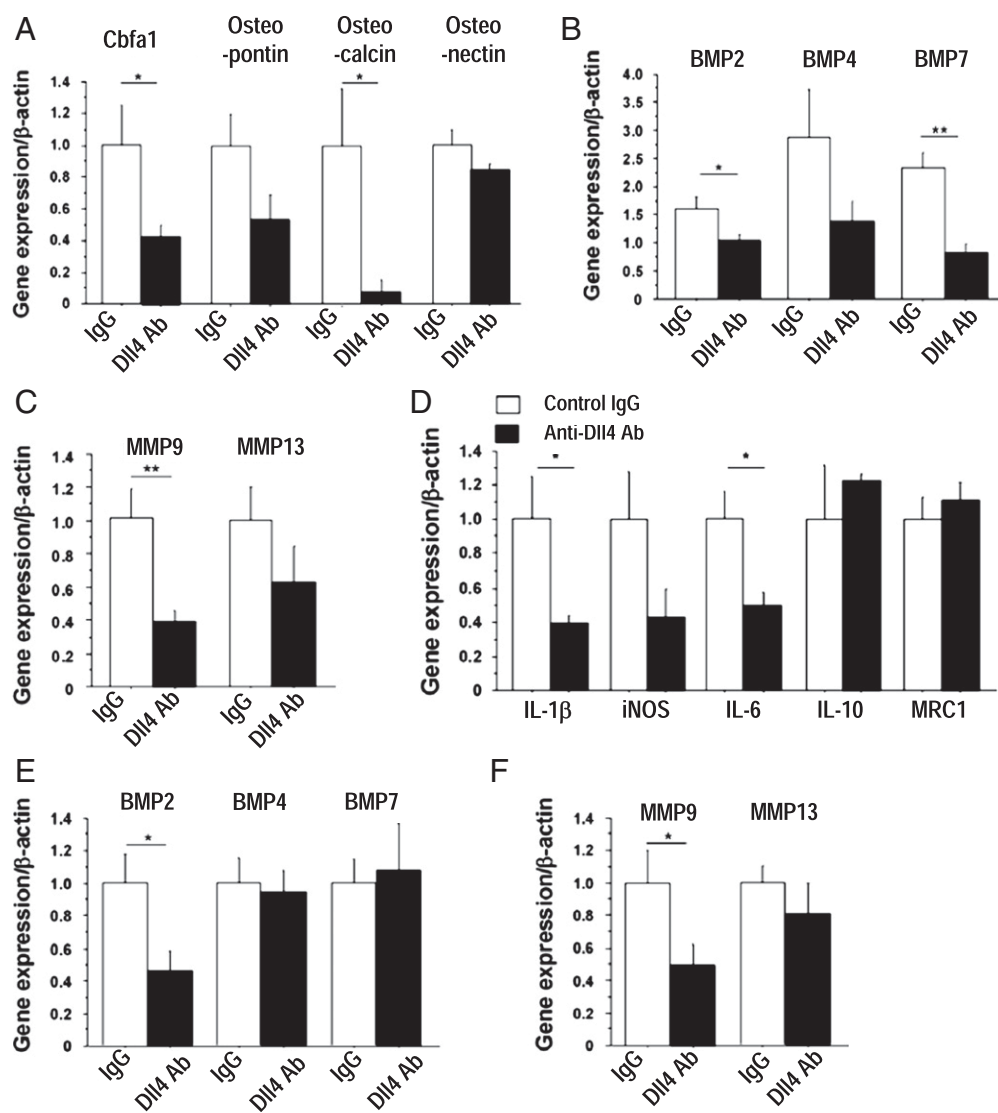


Fig. 3. Role of Dll4 in the expression of osteogenic regulators, MMPs, and inflammatory molecules. (A–C) Quantitative RT-PCR analysis of osteogenic regulators (A), BMPs (B), and MMPs (C) in aortas. (D) Quantitative RT-PCR analyses of the expression of inflammatory molecules in aortas. (E and F) Quantitative RT-PCR analyses of BMPs (E) and MMPs (F) in peritoneal macrophages. A–F show early-phase treatment ($n = 7–8$). * $P < 0.05$; ** $P < 0.01$. All values are mean \pm SEM.

tended to increase GLUT4, C/EBP α , and IRS-1 expression in adipose tissues (SI Appendix, Fig. S6 A and B).

Dll4 Blockade Decreases Macrophage Accumulation in Fat. Insulin resistance associates with increased macrophage accumulation in adipose tissue (2). Late-phase Dll4 Ab administration decreased the numbers of macrophages found in adipose tissue (Fig. 5 F and G). Although early-phase Dll4 blockade did not reduce excessive weight gain or fat mass, it tended to decrease fat macrophage accumulation (SI Appendix, Fig. S6C). Adipose tissue in Ab-treated animals also expressed lower levels of proinflammatory molecules, including MCP-1 (Fig. 5H).

To bolster *in vivo* evidence for the role of Dll4 in macrophage accumulation, we also studied leptin-deficient (*Lep^{ob}/Lep^{ob}*) mice, another commonly used model of metabolic disorders. Dll4 Ab treatment reduced MCP-1 expression and macrophage accumulation in fat tissues (SI Appendix, Fig. S7 A–C). Although Ab treatment did not affect total body weight gain, fat weight was significantly lower in the Ab-treated group (SI Appendix, Fig. S7 D and E), and, as in *Ldlr^{-/-}* mice, Dll4 blockade reduced serum insulin levels (SI Appendix, Fig. S7F).

Dll4 Blockade Reduces MCP-1 Expression. Early-phase and late-phase Dll4 Ab administration decreased expression of MCP-1 in atheromata (Figs. 2B and 6A and SI Appendix, Fig. S2A) and in

adipose tissue (Figs. 5H and 6B). Furthermore, Ab treatment reduced MCP-1 expression in adipocytes and the stromal vascular fraction (SVF) isolated from epididymal fat (adipocytes, $P = 0.04$; SVF, $P = 0.06$) (Fig. 6C). Dll4 blockade decreased expression of the prototypical Notch target gene *Hey1* in adipocytes (SI Appendix, Fig. S4B). MCP-1 levels in the peripheral blood of Ab-treated mice were also lower than in control animals from both treatment protocols (Fig. 6D).

We then asked whether Dll4-Notch signaling regulates MCP-1 expression in RAW264.7 cells and differentiated 3T3-L1 adipocytes. RNAi silencing of Dll4 reduced MCP-1 RNA expression in both cell types (Fig. 6 E and I and SI Appendix, Fig. S8 A and B). In contrast, Dll4 overexpression enhanced MCP-1 expression (Fig. 6 F and J). We also cultured these cells on dishes coated with mouse rDll4 (immobilized rDll4) (34), which increased MCP-1 expression at the RNA and protein levels (Fig. 6 G, H, K, and L). We previously reported that Dll4 ligation activates Notch signaling in human macrophages (13). Here, we show that rDll4 triggers activation of Notch signaling in differentiated 3T3-L1 adipocytes as gauged via Notch reporter gene activity, which was suppressed by Dll4 Ab (SI Appendix, Fig. S8C). This result also revealed that our anti-Dll4 Ab inhibits Dll4 binding. Furthermore, rDll4 promoted expression of MCP-1 in human saphenous vein endothelial cells, an effect that was ab-

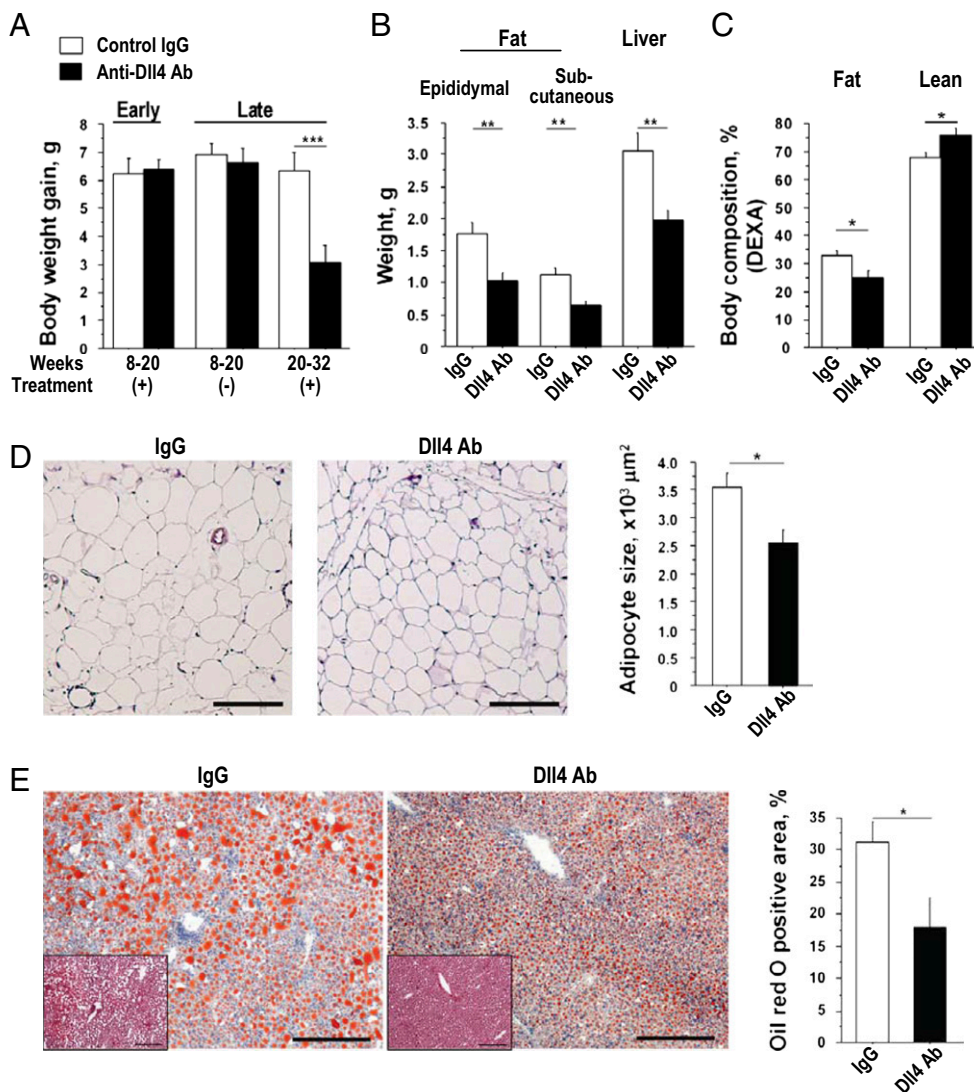


Fig. 4. Effects of Dll4 blockade on fat accumulation. (A) Differences in body weight gain during the study periods (early-phase treatment, $n = 7-8$; late-phase treatment, $n = 19-20$). (B) Weight of fat and liver (late-phase treatment, $n = 19-20$). (C) Results of dual-energy X-ray absorptiometry (DEXA), $n = 5-6$. (D) H&E staining and quantification of adipocyte size in epididymal fat ($n = 7$). (Scale bar: 200 μm .) (E) Oil red O staining of the liver and quantification of lipid deposition (late-phase treatment, $n = 9-10$). (Insets) H&E staining. (Scale bar: 100 μm .) * $P < 0.05$; ** $P < 0.01$; *** $P < 0.001$. All values are mean \pm SEM.

rogated by anti-human Dll4 Ab or DAPT, a γ -secretase inhibitor (SI Appendix, Fig. S8D).

Nuclear factor- κ B (NF- κ B) activates MCP-1 transcription (35, 36). Treatment of RAW264.7 cells and 3T3L-1 adipocytes with rDll4 decreased the levels of the NF- κ B inhibitor I κ B α , indicative of NF- κ B activation (Fig. 6 M and O). SN50, a cell-permeable peptide inhibitor of NF- κ B, abrogated Dll4-triggered MCP-1 induction in both cell types (Fig. 6 N and P). These experiments suggest that stimulation of the NF- κ B pathway and MCP-1 expression in macrophages and adipocytes involve Dll4-mediated signaling, in part. Furthermore, our *in vivo* experiments revealed that Dll4 Ab treatment increased I κ B α levels in the aorta and epididymal fat, consistent with inhibition of NF- κ B (Fig. 6 Q and R).

Dll4 Blockade Attenuates the Proinflammatory Phenotype of Macrophages. The concept is emerging that monocytes/macrophages can be polarized to favor inflammation (Ly6C-high monocytes or “M1” macrophages) or to suppress inflammation (Ly6C-low monocytes or “M2” macrophages). In addition to increasing in number, macrophages that accumulate in tissues in the cardiometabolic syndrome are phenotypically skewed by unknown factors toward the proinflammatory M1 phenotype (37–40). To explore whether Dll4 blockade affects macrophage polarization, we studied the effects of Dll4 blockade on monocytes/macro-

phages by flow cytometry, using SVF obtained from epididymal fat. Ab administration tended to decrease the Ly6C-high population (Fig. 7 A and B), but had no effect on this population in the blood and bone marrow (Fig. 7C). Flow cytometry analyses also showed no significant differences in the percentage of peripheral blood monocytes in *Ldlr*^{-/-} mice treated with Dll4 Ab or IgG (IgG group vs. Ab group: $29.3 \pm 11.6\%$ vs. $27.4 \pm 6.8\%$), suggesting that Dll4 blockade does not deplete circulating monocytes. Furthermore, F4/80-positive macrophages collected from SVF of Ab-treated animals tended to express lower levels of proinflammatory mediators, including iNOS, and slightly higher levels of antiinflammatory mediators such as IL-10 (Fig. 7D).

Macrophages take up lipids, become foam cells in vasculature, and secrete various inflammatory cytokines, accelerating the development of atherosclerosis (41, 42). In this study, Dll4 Ab treatment markedly decreased lipid accumulation in peritoneal macrophages, as determined by Oil red O staining (Fig. 7 E and F). Furthermore, expression of scavenger receptor-A RNA was lower in peritoneal macrophages obtained from Ab-treated mice than in those from control mice (Fig. 7G).

We used RAW264.7 cells to study further the mechanisms underlying the observed proinflammatory role of Dll4. RNAi silencing with Dll4 siRNA decreased expression of typical proinflammatory M1 mediators (e.g., iNOS and TNF- α) and increased expression of mannose receptor 1 (MRC1), an M2 macrophage

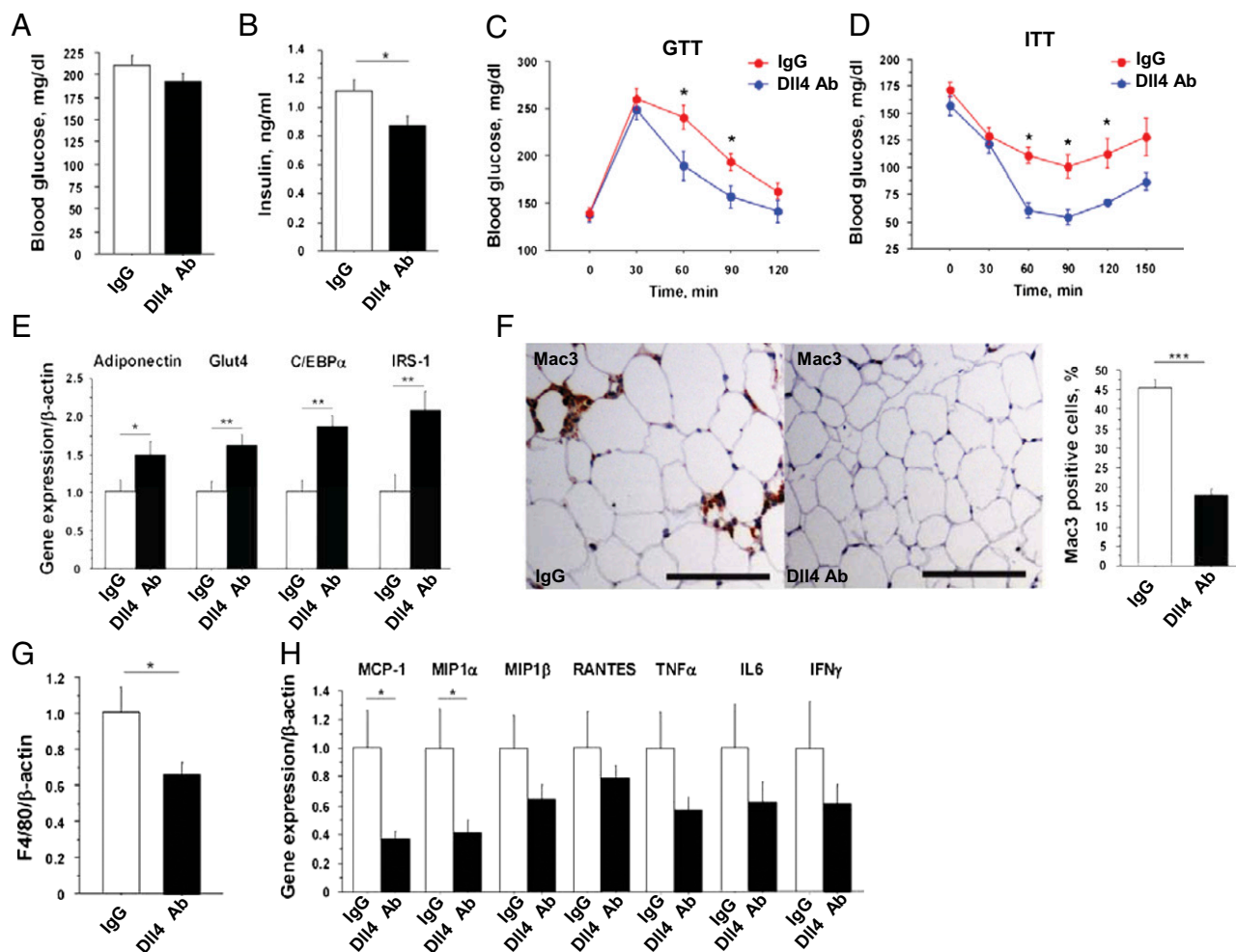


Fig. 5. Effects of Dll4 blockade on insulin sensitivity and macrophage accumulation in fat tissue. (A and B) Blood glucose levels (A) and serum insulin levels (B) after 4-h fasting ($n = 9$). (C and D) Glucose tolerance test (GTT) after 16-h fasting and insulin tolerance test (ITT) after 4-h fasting ($n = 7$). (E) Quantitative RT-PCR analyses of genes related to insulin sensitivity in epididymal fat ($n = 9-10$). (F) Mac3 staining and population of Mac3-positive cells in epididymal fat ($n = 9-10$). (Scale bar: 100 μm .) (G) Quantitative RT-PCR analysis of F4/80 in epididymal fat ($n = 9-10$). (H) Quantitative RT-PCR analyses of expression of chemokines and cytokines in epididymal fat ($n = 9-10$). All data are from late-phase treatment. * $P < 0.05$; ** $P < 0.01$; *** $P < 0.001$. All values are mean \pm SEM.

marker (Fig. 7H). In contrast, enforced Dll4 expression increased iNOS expression and suppressed IL-10 (Fig. 7I). Furthermore, stimulation with immobilized rDll4 increased proinflammatory IL-1 β and iNOS and decreased IL-10 (Fig. 7J). Collectively, these results suggest that Dll4-mediated Notch signaling shifts macrophages toward a proinflammatory phenotype.

Discussion

Accumulating evidence supports the premise that chronic inflammation is central to the pathobiology of atherosclerotic vascular disease and metabolic disorders (2, 25). Regulation of the circulatory, metabolic, and immune systems is highly integrated. Dissecting the multiple intertwined mechanisms for cardiometabolic disorders and developing new therapies for their common pathway thus require well-defined, relevant models (25, 43). The present study demonstrates that inhibition of Dll4, one of the Notch ligands, reduces vascular and adipose inflammation, possibly through the effects on NF- κ B/MCP-1-mediated responses—implicating Dll4 as an important instigator of the cardiometabolic syndrome. Our in vivo and in vitro results indicate the expression of Dll4 in multiple cell types and its function related to the development of the cardiometabolic syndrome. Whereas genetic manipulation—such as cell-type-specific loss-of-function and/or gain-of-function mouse strains—may provide insight into the

relative contribution of each cell type to Dll4-mediated cardiometabolic inflammation, systemic administration of well-characterized anti-Dll4 Ab provides clinically translatable proof of concept for the role of Dll4 in the shared mechanisms for cardiometabolic syndrome and facilitates the development of new biotherapies for this disease. Our study demonstrates that Dll4 blockade using our Ab improves the cardiometabolic syndrome and represents clinically relevant evidence that Dll4 can be a therapeutic target.

This study suggests that Dll4 induces MCP-1 expression in arteries and adipose tissues. MCP-1 plays a key role in monocyte/macrophage recruitment and in macrophage-dependent inflammatory responses that lead to the development of atherosclerosis and insulin resistance (44, 45). Our in vitro experiments demonstrate that Dll4 can induce MCP-1 expression in several cell types responsible for the development of cardiometabolic disorders. In the present study, Dll4 blockade reduced MCP-1 levels in the aorta, fat tissues, and peripheral blood. Enhanced expression of MCP-1 by Dll4 in atheromata and adipose tissues can promote accumulation of macrophages, another major source of MCP-1. Dll4-Notch signaling may thus amplify macrophage accumulation through the induction of MCP-1 expression, an effect that Dll4 inhibition appears to reverse.

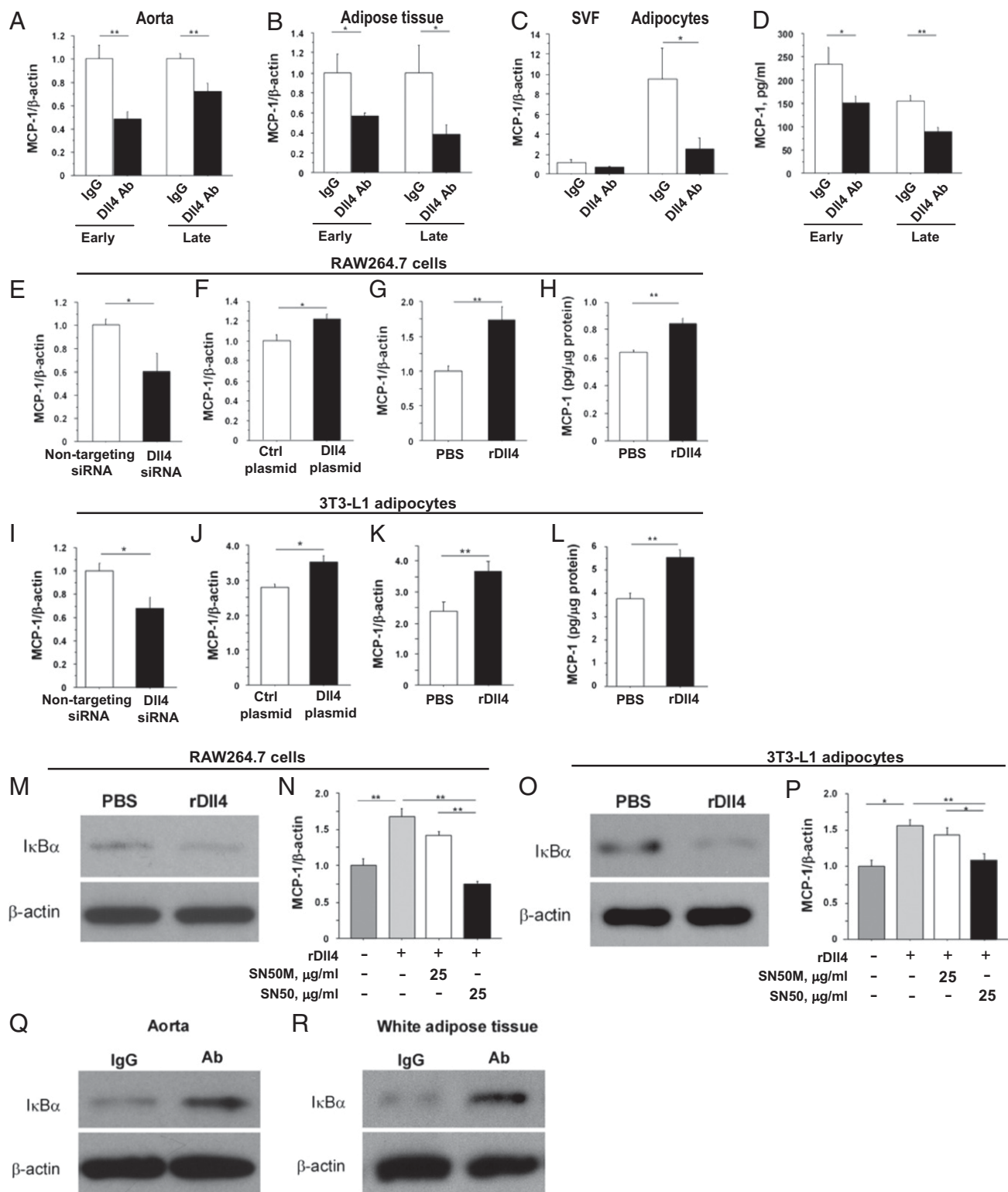


Fig. 6. Role of DII4 in MCP-1 expression in vivo and in vitro. (A and B) MCP-1 RNA expression in aortas (A) and fat tissue (B). (C) MCP-1 RNA expression in SVF and adipocytes obtained from epididymal fat. (D) Serum MCP-1 levels. Early-phase treatment, $n = 7-8$; late-phase treatment, $n = 9-10$. (E-G) Effects of RNAi silencing of DII4 (E), transfection of plasmid encoding DII4 (F), and stimulation with immobilized rDII4 (G) on MCP-1 RNA expression in RAW264.7 cells. (H) MCP-1 protein levels in supernatant of rDII4-treated RAW264.7 cells. (I-K) Effects of RNAi silencing of DII4 (I), transfection of plasmid encoding DII4 (J), and stimulation with immobilized rDII4 (K) on MCP-1 RNA expression in 3T3-L1 adipocytes. (L) MCP-1 protein levels in supernatant of rDII4-treated 3T3-L1 adipocytes. (M) Degradation of I κ B α in rDII4-stimulated RAW264.7 cells. (N) Reduction of MCP-1 expression by NF- κ B inhibitor SN50 in rDII4-stimulated RAW264.7 cells. SN50M, inactive control for SN50. (O) Degradation of I κ B α in rDII4-stimulated 3T3-L1 adipocytes. (P) Reduction of MCP-1 expression by NF- κ B inhibitor SN50 in rDII4-stimulated 3T3-L1 adipocytes. (Q and R) Inhibition of NF- κ B in aortas (Q) and fat tissues (R) determined by degradation of I κ B α in DII4 Ab-treated *Ldlr*^{-/-} mice. E-P, $n = 6$. Q and R show representative data from late-phase treatment, $n = 4$. * $P < 0.05$; ** $P < 0.01$. All values are mean \pm SEM.

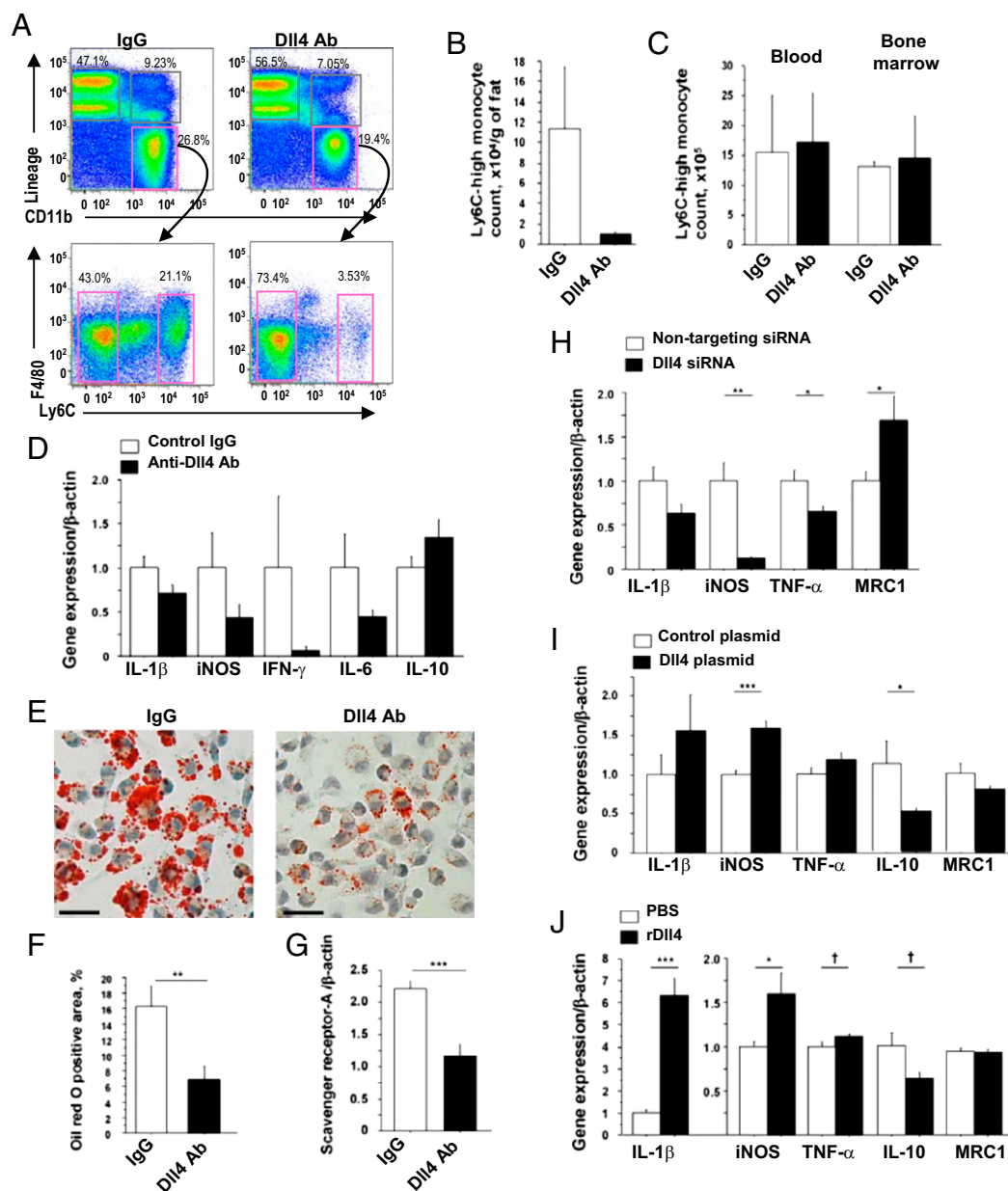


Fig. 7. Role of DII4 in proinflammatory activation of macrophages. (A) Flow cytometry analyses of SVF obtained from epididymal fat. (B) Count of Ly6C-high monocytes in fat. (C) Ly6C-high monocyte population in blood and bone marrow. (D) Quantitative RT-PCR analyses of expression of inflammatory molecules in F4/80-positive macrophages obtained from fat. (E and F) Oil red O staining (E) and quantification of lipid deposition (F) of peritoneal macrophages obtained from *Ldlr*^{-/-} mice that received late-phase treatment. (G) Quantitative RT-PCR analyses of expression of macrophage scavenger receptor-A in peritoneal macrophages. (H–J) Effects of RNAi silencing of DII4 (H), overexpression of DII4 using expressing plasmid (I), and stimulation with immobilized rDII4 (J) on the expression of inflammatory molecules in RAW264.7 cells. A–C, $n = 3$; D–G, $n = 9–10$; H–J, $n = 6$. [†] $P < 0.05$; * $P < 0.05$; ** $P < 0.01$; *** $P < 0.001$. All values are mean \pm SEM.

Excessive polarization of macrophages toward a proinflammatory state may contribute to the pathogenesis of the cardiometabolic syndrome (46, 47). Proinflammatory macrophage polarization may induce atherogenesis and plaque destabilization through collagen loss and calcification in plaques (25, 27, 48) and the development of adipose inflammation and insulin resistance (37). The concept of M1/M2 macrophage balance was developed in vitro, as gauged by the expression of inflammatory mediators. Recent evidence suggests a wide range of monocyte/macrophage heterogeneity in response to either innate or adaptive immune signals (49). Despite accumulating in vitro evidence and its large clinical impact, in vivo mechanisms for macrophage activation remain incompletely understood (50). Several lines of in vivo and in vitro evidence in the present study demonstrate that DII4

induces expression of genes associated with the proinflammatory M1 phenotype. Assuming that macrophages have plasticity, local microenvironmental cues may tip the M1/M2 balance. Alternatively, distinct subsets of circulating monocytes may be committed to particular M1/M2 fates. Although Notch signaling is required for the appearance of hematopoietic stem cells during early development, canonical Notch signaling is not required for the generation of myeloid cells from hematopoietic stem cells (51). Similarly, in this study, DII4 blockade did not alter monocyte numbers and/or the Ly-6C-high monocyte subpopulation, which is generally considered to be proinflammatory, in the blood and bone marrow. Thus, DII4 may trigger the proinflammatory activation of macrophages in lesions.

Our results suggest that Dll4-Notch signaling augments NF- κ B activation. How Notch signaling leads to NF- κ B activation is poorly understood (13, 52–55). We and others have suggested the intertwined crosstalk between NF- κ B and Notch pathways. Our previous study reported that proinflammatory stimuli (e.g., IL-1 β , minimally modified LDL, and LPS) induce Dll4 expression in cultured human macrophages in a manner dependent on the Toll-like receptor/IL-1 receptor superfamily and NF- κ B and that Dll4 promotes NF- κ B activation, leading to the expression of NF- κ B-regulated genes, such as iNOS and Dll4 itself (13). The present study indicates *in vivo* and *in vitro* that Dll4-Notch mediates MCP-1 induction, in part via NF- κ B activation, which leads to increases of many proinflammatory genes, including MCP-1, iNOS, and MMP-9, all of which were induced by Dll4 in this study. Interaction of Notch intracellular domains and NF- κ B pathway components is complex, appears to be context and cell-type dependent, and generally remains unclear. Because activation of NF- κ B represents the proinflammatory M1 environment and contributes to atherosclerosis, insulin resistance, and obesity (38, 56, 57), its interplay with Dll4-Notch signaling deserves further investigation. Furthermore, our results suggest that the Dll4-Notch axis promotes sustained macrophage activation via a positive feedback loop—a vicious cycle that represents mechanisms for uncontrolled macrophage activation typical of chronic inflammatory diseases. Overall, our results are consistent with the intriguing possibility that the Dll4-Notch axis serves as a key regulator of macrophage activation *in vivo*.

Here we report that Dll4 blockade lessens the accumulation of macrophages, decreases fat mass, and abrogates insulin resistance in two models of metabolic disorders. Our *in vivo* and *in vitro* experiments fall short of providing definitive causal relationships between these three complex parameters. Reduced adipose accumulation in these animals might help improve insulin resistance and reduce macrophage accumulation, but data from the early-phase and late-phase treatments suggest that Dll4 blockade modulates the expression of proinflammatory factors in fat before fat weight reduction. Furthermore, several studies reported that macrophage accumulation in fat precedes the development of insulin resistance in mice (58–60). Our finding that Dll4 Ab treatment reduced expression of M1 gene products and improved insulin resistance agrees with the recent evidence that accumulation of proinflammatory macrophages leads to the development of insulin resistance (61, 62). MCP-1 also directly affects adipocyte function and insulin sensitivity (44, 63) and participates in the development of fatty liver (64). We therefore speculate that reduction of MCP-1 by Dll4 blockade, observed in multiple cell types, also contributes to the improvement of insulin sensitivity. Dll4 blockade disrupts angiogenesis and inhibits cancer growth by induction of hypoxia (10–12), and evidence links angiogenesis with adipose tissue development (65), fat accumulation, and insulin resistance (66). Therefore, the antiangiogenic effects of Dll4 blockade also may have contributed to the results reported here. Further studies are needed to tease out the mechanisms underlying the effects of Dll4 blockade on adipose tissue inflammation and insulin resistance.

Whereas global Notch inhibition (e.g., γ -secretase inhibitors) has acutely toxic effects (24), selective Dll4 inhibition produced no signs of distress or toxicity in our mice. Furthermore, we did not observe significant differences in body weight gain in mice that received 12 wk of the early-phase administration of Dll4 Ab or IgG group (8–20 wk of age), whereas late-phase Dll4 blockade (20–32 wk of age) retarded excessive fat accumulation. The effects during the late-phase treatment may account for increased Dll4 expression in adipose tissue in fat-fed *Ldlr*^{-/-} mice over time. Dll4 expression in 3T3-L1 adipocytes also increased during differentiation *in vitro* (SI Appendix, Fig. S8E). Although a recent study suggested that long-term (12 wk) Dll4 blockade can induce adverse effects in the liver in mice (67), our Dll4 Ab treatment for 12 wk attenuated fatty liver. The same study also reported the formation of vascular neoplasm by Dll4 Ab administration (67). In our study, two authors independently and thoroughly examined organs such as the aorta, adipose tissue, liver, and small intestine.

We did not find any signs of vascular neoplasm-like changes in our Ab-treated mice. Differences in several factors (e.g., mouse strains, antibodies, and routes of administration) might have caused these differences. Nevertheless, the feasibility of long-term Dll4 blockade needs to be established by further evaluations.

In summary, our study demonstrates that Notch signaling drives proinflammatory programs of gene expression associated with cardiometabolic syndrome. Dll4 appears to function in homotypic and heterotypic crosstalk between pathways that control central elements of inflammatory and metabolic responses in macrophages and adipocytes, and thus constitutes a unique therapeutic target in cardiometabolic disorders.

Materials and Methods

Mice and Anti-Dll4 Ab Treatment. *Ldlr*^{-/-} mice were fed a high-fat, high-cholesterol diet (D12108; Research Diets) from 8 wk of age through the completion of the study. *Lep*^{ob}/*Lep*^{ob} mice and Notch reporter transgenic mice were fed normal chow. Animal care and experimentation were approved by the Harvard Medical School Institutional Animal Care and Use Committee. Mice were treated with well-characterized hamster-derived anti-mouse Dll4 antibody (14–20). *Ldlr*^{-/-} mice were injected with 250 μ g of anti-mouse Dll4 antibody or isotype control IgG (BioXcell) intraperitoneally twice a week from 8 wk of age (early phase) or from 20 wk of age (late phase) for 12 wk. For *Lep*^{ob}/*Lep*^{ob} mice, the amount of Dll4 Ab and IgG was adjusted according to body weight (10 μ g/g) and administered for 10 wk. Mice were weighed twice a week. For bolus injection, we administered 250 μ g of Dll4 Ab or IgG to fat-fed 10-wk-old *Ldlr*^{-/-} mice or Notch reporter transgenic mice and harvested them at 6 h after injection.

Ex Vivo Fluorescence Reflectance Imaging of the Aorta and Aortic Valve. *Ldlr*^{-/-} mice that received late-phase treatment were used for fluorescence reflectance imaging. Two spectrally distinct near-infrared fluorescent agents were administered to each mouse 24 h before imaging—cross-linked iron oxide fluorescent iron nanoparticles for detection of macrophage accumulation (CLIO750, 750 nm), and OsteoSense680 for detection of osteogenic activity (680 nm; VisEn). The detailed method was described previously (68).

Analysis of Metabolic Parameters. Glucose and insulin tolerance tests were performed after 16-h and 4-h fasting, respectively. Glucose and insulin solutions were injected into the peritoneal cavity at doses of 1.0 g/kg and 0.5 unit/kg, respectively. Indirect calorimetry and physical activity measurements using *Ldlr*^{-/-} mice were performed at the end of 12 wk of late-phase treatment. The details of indirect experiments were described previously (69).

Flow Cytometry Analysis. To investigate effects of Dll4 blockade on monocytes/macrophages and circulating leukocytes, we performed flow cytometry analysis using SVF, bone marrow, and peripheral blood leukocytes. Antibodies used in this study are described in SI Appendix.

Cell Culture Experiments. To activate Dll4-mediated Notch signaling, we seeded RAW264.7 cells, differentiated 3T3-L1 adipocytes, and human saphenous vein endothelial cells to plates coated with recombinant mouse or human Dll4 (immobilized rDll4) (R&D Systems) (34). Day 10 3T3-L1 adipocytes were used as differentiated 3T3-L1 adipocytes. We transfected siRNA against mouse Dll4 (Dharmacon) and plasmid encoding mouse Dll4 (GeneCopoeia) to RAW264.7 cells and 3T3-L1 adipocytes and RBP-J κ reporter (SABiosciences) to 3T3-L1 adipocytes by electroporation (Nucleofector system; Amaxa), according to the manufacturer's instructions.

Statistics. Data are expressed as mean \pm SEM for continuous variables. Comparisons between two groups were performed by unpaired Student's *t* test. Comparisons of multiple groups were made by one-way ANOVA, followed by the Student-Newman-Keuls multiple-comparison test. *P* values <0.05 were considered statistically significant.

For further details, please refer to SI Appendix.

ACKNOWLEDGMENTS. We thank Jose-Luiz Figueiredo, Eugenia Shvartz, Yevgenia Tesmenitsky, Jacob Aaron, and Mohammad Zafari for technical assistance, and Sara Karwacki for her editorial expertise. This study was supported in part by National Institutes of Health Grant R01HL107550 (to M.A.) and American Heart Association Grants 0655878T (to M.A.) and 0835460N (to E.A.), Postdoctoral Fellowship Awards for Research Abroad from the Japanese Heart Foundation, the Japan Society for the Promotion of Science, and the Uehara Memorial Foundation (D.F.).

1. Eckel RH, Grundy SM, Zimmet PZ (2005) The metabolic syndrome. *Lancet* 365: 1415–1428.
2. Hotamisligil GS (2006) Inflammation and metabolic disorders. *Nature* 444:860–867.
3. Artavanis-Tsakonas S, Rand MD, Lake RJ (1999) Notch signaling: Cell fate control and signal integration in development. *Science* 284:770–776.
4. Aster JC, Pear WS, Blacklow SC (2008) Notch signaling in leukemia. *Annu Rev Pathol* 3: 587–613.
5. Radtke F, Fasnacht N, Macdonald HR (2010) Notch signaling in the immune system. *Immunity* 32:14–27.
6. Hao L, et al. (2010) Notch-1 activates estrogen receptor- α -dependent transcription via IKK α in breast cancer cells. *Oncogene* 29:201–213.
7. Ranganathan P, Weaver KL, Capobianco AJ (2011) Notch signalling in solid tumours: A little bit of everything but not all the time. *Nat Rev Cancer* 11:338–351.
8. Pajvani UB, et al. (2011) Inhibition of Notch signaling ameliorates insulin resistance in a FoxO1-dependent manner. *Nat Med* 17:961–967.
9. Rubio-Aliaga I, et al. (2009) Dll1 haploinsufficiency in adult mice leads to a complex phenotype affecting metabolic and immunological processes. *PLoS ONE* 4:e6054.
10. Noguera-Troise I, et al. (2006) Blockade of Dll4 inhibits tumour growth by promoting non-productive angiogenesis. *Nature* 444:1032–1037.
11. Ridgway J, et al. (2006) Inhibition of Dll4 signalling inhibits tumour growth by deregulating angiogenesis. *Nature* 444:1083–1087.
12. Thurston G, Noguera-Troise I, Yancopoulos GD (2007) The Delta paradox: DLL4 blockade leads to more tumour vessels but less tumour growth. *Nat Rev Cancer* 7: 327–331.
13. Fung E, et al. (2007) Delta-like 4 induces notch signaling in macrophages: Implications for inflammation. *Circulation* 115:2948–2956.
14. Moriyama Y, et al. (2008) Delta-like 1 is essential for the maintenance of marginal zone B cells in normal mice but not in autoimmune mice. *Int Immunol* 20:763–773.
15. Fukushima A, et al. (2008) Notch ligand Delta-like4 inhibits the development of murine experimental allergic conjunctivitis. *Immunol Lett* 121:140–147.
16. Sekine C, et al. (2009) Differential regulation of splenic CD8⁺ dendritic cells and marginal zone B cells by Notch ligands. *Int Immunol* 21:295–301.
17. Yamanda S, et al. (2009) Role of ephrinB2 in nonproductive angiogenesis induced by Delta-like 4 blockade. *Blood* 113:3631–3639.
18. Kassan N, et al. (2010) Cutting edge: Plasmacytoid dendritic cells induce IL-10 production in T cells via the Delta-like-4/Notch axis. *J Immunol* 184:550–554.
19. Koyanagi A, Sekine C, Yagita H (2012) Expression of Notch receptors and ligands on immature and mature T cells. *Biochem Biophys Res Commun* 418:799–805.
20. Oishi H, et al. (2010) Blockade of delta-like ligand 4 signaling inhibits both growth and angiogenesis of pancreatic cancer. *Pancreas* 39:897–903.
21. Subramanian S, et al. (2008) Dietary cholesterol worsens adipose tissue macrophage accumulation and atherosclerosis in obese LDL receptor-deficient mice. *Arterioscler Thromb Vasc Biol* 28:685–691.
22. Gale NW, et al. (2004) Haploinsufficiency of delta-like 4 ligand results in embryonic lethality due to major defects in arterial and vascular development. *Proc Natl Acad Sci USA* 101:15949–15954.
23. Duncan AW, et al. (2005) Integration of Notch and Wnt signaling in hematopoietic stem cell maintenance. *Nat Immunol* 6:314–322.
24. Fre S, et al. (2005) Notch signals control the fate of immature progenitor cells in the intestine. *Nature* 435:964–968.
25. Aikawa M, Libby P (2004) The vulnerable atherosclerotic plaque: Pathogenesis and therapeutic approach. *Cardiovasc Pathol* 13:125–138.
26. Libby P, Aikawa M (2002) Stabilization of atherosclerotic plaques: New mechanisms and clinical targets. *Nat Med* 8:1257–1262.
27. Aikawa E, et al. (2009) Arterial and aortic valve calcification abolished by elastolytic cathepsin S deficiency in chronic renal disease. *Circulation* 119:1785–1794.
28. Shao JS, Cheng SL, Sadhu J, Towler DA (2010) Inflammation and the osteogenic regulation of vascular calcification: A review and perspective. *Hypertension* 55: 579–592.
29. New SE, Aikawa E (2011) Molecular imaging insights into early inflammatory stages of arterial and aortic valve calcification. *Circ Res* 108:1381–1391.
30. Shimizu T, et al. (2009) Notch signaling induces osteogenic differentiation and mineralization of vascular smooth muscle cells: Role of Mx2 gene induction via Notch-RBP-Jk signaling. *Arterioscler Thromb Vasc Biol* 29:1104–1111.
31. Feig JE, et al. (2011) Reversal of hyperlipidemia with a genetic switch favorably affects the content and inflammatory state of macrophages in atherosclerotic plaques. *Circulation* 123:989–998.
32. Towler DA (2008) Oxidation, inflammation, and aortic valve calcification peroxide paves an osteogenic path. *J Am Coll Cardiol* 52:851–854.
33. Deguchi JO, et al. (2005) Matrix metalloproteinase-13/collagenase-3 deletion promotes collagen accumulation and organization in mouse atherosclerotic plaques. *Circulation* 112:2708–2715.
34. Williams CK, Li JL, Murga M, Harris AL, Tosato G (2006) Up-regulation of the Notch ligand Delta-like 4 inhibits VEGF-induced endothelial cell function. *Blood* 107: 931–939.
35. Jiao P, et al. (2009) Obesity-related upregulation of monocyte chemotactic factors in adipocytes: Involvement of nuclear factor- κ B and c-Jun NH2-terminal kinase pathways. *Diabetes* 58:104–115.
36. Shin WS, Szuba A, Rockson SG (2002) The role of chemokines in human cardiovascular pathology: Enhanced biological insights. *Atherosclerosis* 160:91–102.
37. Chawla A (2010) Control of macrophage activation and function by PPARs. *Circ Res* 106:1559–1569.
38. Mantovani A, Garlanda C, Locati M (2009) Macrophage diversity and polarization in atherosclerosis: A question of balance. *Arterioscler Thromb Vasc Biol* 29:1419–1423.
39. Gordon S (2007) Macrophage heterogeneity and tissue lipids. *J Clin Invest* 117:89–93.
40. Ley K, Miller YI, Hedrick CC (2011) Monocyte and macrophage dynamics during atherogenesis. *Arterioscler Thromb Vasc Biol* 31:1506–1516.
41. Suzuki H, et al. (1997) A role for macrophage scavenger receptors in atherosclerosis and susceptibility to infection. *Nature* 386:292–296.
42. Parthasarathy S, Steinberg D, Witztum JL (1992) The role of oxidized low-density lipoproteins in the pathogenesis of atherosclerosis. *Annu Rev Med* 43:219–225.
43. Williams KJ, Feig JE, Fisher EA (2008) Rapid regression of atherosclerosis: Insights from the clinical and experimental literature. *Nat Clin Pract Cardiovasc Med* 5:91–102.
44. Kanda H, et al. (2006) MCP-1 contributes to macrophage infiltration into adipose tissue, insulin resistance, and hepatic steatosis in obesity. *J Clin Invest* 116:1494–1505.
45. Liang CP, Han S, Senokuchi T, Tall AR (2007) The macrophage at the crossroads of insulin resistance and atherosclerosis. *Circ Res* 100:1546–1555.
46. Swirski FK, et al. (2007) Ly-6Chi monocytes dominate hypercholesterolemia-associated mononitrosylation and give rise to macrophages in atheroma. *J Clin Invest* 117:195–205.
47. Tacke F, et al. (2007) Monocyte subsets differentially employ CCR2, CCR5, and CX3CR1 to accumulate within atherosclerotic plaques. *J Clin Invest* 117:185–194.
48. Shanahan CM (2007) Inflammation ushers in calcification: A cycle of damage and protection? *Circulation* 116:2782–2785.
49. Mosser DM, Edwards JP (2008) Exploring the full spectrum of macrophage activation. *Nat Rev Immunol* 8:958–969.
50. Hotamisligil GS (2010) Endoplasmic reticulum stress and the inflammatory basis of metabolic disease. *Cell* 140:900–917.
51. Yuan JS, Kousis PC, Suliman S, Visan I, Guidos CJ (2010) Functions of notch signaling in the immune system: Consensus and controversies. *Annu Rev Immunol* 28:343–365.
52. Osipo C, Golde TE, Osborne BA, Miele LA (2008) Off the beaten pathway: The complex cross talk between Notch and NF- κ B. *Lab Invest* 88:11–17.
53. Vacca A, et al. (2006) Notch3 and pre-TCR interaction unveils distinct NF- κ B pathways in T-cell development and leukemia. *EMBO J* 25:1000–1008.
54. Monsalve E, et al. (2009) Notch1 upregulates LPS-induced macrophage activation by increasing NF- κ B activity. *Eur J Immunol* 39:2556–2570.
55. Palaga T, et al. (2008) Notch signaling is activated by TLR stimulation and regulates macrophage functions. *Eur J Immunol* 38:174–183.
56. Gao Z, et al. (2002) Serine phosphorylation of insulin receptor substrate 1 by inhibitor κ B kinase complex. *J Biol Chem* 277:48115–48121.
57. Hess K, Ushmorov A, Fiedler J, Brenner RE, Wirth T (2009) TNF α promotes osteogenic differentiation of human mesenchymal stem cells by triggering the NF- κ B signaling pathway. *Bone* 45:367–376.
58. Suganami T, Ogawa Y (2010) Adipose tissue macrophages: Their role in adipose tissue remodeling. *J Leukoc Biol* 88:33–39.
59. Weisberg SP, et al. (2003) Obesity is associated with macrophage accumulation in adipose tissue. *J Clin Invest* 112:1796–1808.
60. Xu H, et al. (2003) Chronic inflammation in fat plays a crucial role in the development of obesity-related insulin resistance. *J Clin Invest* 112:1821–1830.
61. Kang K, et al. (2008) Adipocyte-derived Th2 cytokines and myeloid PPAR δ regulate macrophage polarization and insulin sensitivity. *Cell Metab* 7:485–495.
62. Odegaard JI, et al. (2007) Macrophage-specific PPAR γ controls alternative activation and improves insulin resistance. *Nature* 447:1116–1120.
63. Sartipy P, Loskutoff DJ (2003) Monocyte chemoattractant protein 1 in obesity and insulin resistance. *Proc Natl Acad Sci USA* 100:7265–7270.
64. Rull A, et al. (2009) Hepatic monocyte chemoattractant protein-1 is upregulated by dietary cholesterol and contributes to liver steatosis. *Cytokine* 48:273–279.
65. Cao Y (2007) Angiogenesis modulates adipogenesis and obesity. *J Clin Invest* 117: 2362–2368.
66. Bråkenhielm E, et al. (2004) Angiogenesis inhibitor, TNP-470, prevents diet-induced and genetic obesity in mice. *Circ Res* 94:1579–1588.
67. Yan M, et al. (2010) Chronic DLL4 blockade induces vascular neoplasms. *Nature* 463: E6–E7.
68. Aikawa E, et al. (2007) Multimodality molecular imaging identifies proteolytic and osteogenic activities in early aortic valve disease. *Circulation* 115:377–386.
69. Maeda K, et al. (2005) Adipocyte/macrophage fatty acid binding proteins control integrated metabolic responses in obesity and diabetes. *Cell Metab* 1:107–119.